

The Development and Validation of a Simple Snow Model for the GISS GCM

MARC LYNCH-STIEGLITZ

Goddard Institute for Space Studies, NASA, Department of Geological Sciences, Columbia University, New York, New York

(Manuscript received 2 August 1993, in final form 10 May 1994)

ABSTRACT

Five years of meteorological and hydrological data from a typical New England watershed where winter snow cover is significant were used to drive and validate two off-line land surface schemes suitable for use in the Goddard Institute for Space Studies GCM: a baseline scheme that does not model the physics of a snowpack and therefore, neglects the insulating properties of snow cover; and a modified scheme in which a three-layer snowpack is modeled. Comparing baseline model results with validation data reveals several model deficiencies. Surface radiation temperatures could not adequately be modeled and the ground froze to unreasonable depths. Furthermore, because of ground cooling resulting from large surface heat fluxes to the atmosphere from the uninsulated surface, deeper model layers did not unfreeze until midsummer. As such, the normal hydrologic processes of runoff, ground water infiltration, and movement, etc., are compromised for a good part of the year. With the inclusion of a simple three-layer snow model into the baseline model, not only are the ground and surface radiation temperatures adequately modeled but all the features of snowpack ripening that characterize pack growth/ablation are simulated.

1. Introduction

a. Background

Since the mid-1970s when Charney et al. (1975, 1977) focused attention on the possible feedbacks between the land surface and climate, especially in regard to the continued Sahelian drought, there have been sustained efforts to develop more realistic land-surface schemes for general circulation models (GCMs) that accurately model the transfer of energy and water between the land and atmosphere. However, concurrently, high-resolution meteorological and hydrological datasets that can be used to validate these schemes have not been available. This study is an attempt to bridge the gap between model development and validation, and is the first in a series of papers in which five years of meteorological and hydrological data from a typical New England watershed are used to validate and improve a current off-line working version of the Goddard Institute for Space Studies (GISS) land-surface scheme (Abramopoulos et al. 1988), hereafter referred to as the baseline model.

Both models and data have shown that large areal snow cover has a profound effect on the regional and possibly remote climate via changes in the surface energy balance (Barnett et al. 1989; Namias 1985; Yeh et al. 1983). In addition, snow cover affects the

hydrologic cycle. In many northern latitude regions (such as the state of California) spring meltwater derived from the winter snowpack represents the greatest source for the yearly ground moisture budget (Aguado 1985). Furthermore, in all but permafrost regions, the insulating characteristics of snow are such that only the near-surface ground freezes and deep water drainage is uninterrupted. To account for these effects, any GCM land-surface scheme must properly model the role of the snow cover.

The baseline land-surface scheme does not formally treat the wintertime snowpack as anything other than a moisture store, and as such, both neglects the insulating properties of snow and is inadequate for proper modeling of the surface radiation temperature. This inadequate treatment of the snowpack results in freezing of model ground layers to depths of 2 m in winter for our New England watershed. Further, these deep model layers remain frozen well into spring and midsummer. In reality, because of the presence of prolonged snow cover, ground freezing rarely occurs for the site. As can be imagined, this unrealistic ground freezing has serious consequences for the proper simulation of the hydrologic cycle. Therefore, the focus of this paper is to describe the effort to develop and incorporate a simple snowpack model into the GISS land-surface scheme that can be used to predict ground temperatures, the diurnal surface radiation temperature, and snow cover characteristics (i.e., snowpack mass, heat content, and depth).

Corresponding author address: Marc Lynch-Stieglitz, NASA/GISS, 2880 Broadway, New York, NY 10025.
E-mail: ccmls@nasagiss.nasa.gov

b. Treatment of snow cover in GCMs

Mostly due to computational limitations, GCM snow model development to date has not followed the complex treatments of Anderson (1976) and Jordan (1991) but instead has focused on the development of 1–3 layer moving boundary models with snowpack density assumed constant throughout the pack and a simple parameterization representing mechanical compaction. Both the BATS (Dickinson et al. 1986) and BEST (Pitman et al. 1991) land-surface schemes include three soil layers where, in the presence of a partially or fully snow-covered grid box, and for the purposes of evaluating surface fluxes from the grid box, a composite soil/snow layer is envisioned. Thus, in the absence or presence of snow there are always three model layers. At each time step the average snowpack density is calculated, from which the soil thermal properties, K_{th} (thermal conductivity) and C_v (volumetric specific heat) can be determined. As such, this composite layer has thermal properties that are the weighted means of the snow and bare ground conductivities and heat capacities. To capture the diurnal and seasonal cycle both models use force–restore (Deardorff 1978) methods to calculate ground temperatures. Therefore, heat flow within the soil/snow layers is not physically modeled, and as Dickinson (1988) noted, the force–restore formalism needs considerable modification to account for soil inhomogeneity, including snow cover.

On the other hand, CLASS (Verseghy 1991) employs a single snow layer overlaying the ground, and fluxes in a grid box are computed separately for the bare and snow-covered soil. Fluxes to the atmosphere are then aggregated based on the proportion of the grid box covered by snow. Heat flow within the ground and snow layer is physically modeled via heat diffusion along the thermal gradient. While it is computationally more expensive to keep track of independent snow and bare ground portions in each grid box, the somewhat artificial soil/snow compositing is not necessary in this model. However, as the depth of the snowpack becomes large compared to the thermal damping depth of snow (approximately 6–10 cm) the full diurnal range of the surface radiating temperature cannot be captured and both the calculations for surface fluxes to the atmosphere and the snowpack's ability to insulate the ground become corrupted.

The scheme developed in this study employs three snow layers overlaying the ground, where the top layer thickness is a function of the thermal damping depth of snow and a separate density is calculated for each snow layer. Like the CLASS model, vertical heat flow is modeled via the diffusion equation.

c. Paper outline

The remainder of the paper is outlined as follows. A description of the site input/validation data is given

and the general characteristics and climatology of the watershed are discussed. Descriptions of both the baseline land-surface scheme and a simple snow model that is incorporated into the baseline scheme are given. Site meteorological data is then used to drive the models in an off-line mode, and validation data is used to evaluate model performance.

2. Sleepers river watershed data

This section summarizes an extensive discussion on the Sleepers River watershed given in Anderson (1977).

In 1966 a joint program between the National Oceanic and Atmospheric Administration (NOAA) and the Agricultural Research Service (ARS) was initiated to collect a set of sufficiently high-resolution hydro-meteorological measurements that could be used to better understand snowpack growth/ablation and to evaluate complex snow models (Anderson 1976). The NOAA–ARS snow research station is a 15 acre clearing (mowed bare soil) situated within the W-3 subwatershed of the Sleepers River watershed in the eastern highlands of Vermont. The vegetation surrounding this 15 acre clearing is composed of one-third grassland, one-third coniferous forest, and one-third deciduous forest. At an altitude of 552 m, the snow station's mean annual air temperature of 4.1°C with a standard deviation of 11.4°C is fairly representative of the watershed as a whole. "The frost-free period on the watershed varies from about 95 days at the highest elevation to 130 days at lower elevations. The mean annual precipitation for the W-3 watershed is about 43 inches. The maximum water equivalent of snow cover is normally about 9"–12". Total snow depth averages about 100". In this area of Vermont, constant snow cover usually persists throughout the December–March period with snowmelt occurring in late March and April (Anderson 1977). Because snow cover usually arrives early in the winter season, the ground is highly insulated and ground temperatures near the surface rarely deviate from 0°C with no freezing below approximately 12 cm.

It is a 5-year record of hydro-meteorological measurements taken at this site that will be used to validate and improve the GISS land-surface scheme. The extent of these measurements is shown in Table 1. Two datasets are shown. The first will be used to drive the land-surface scheme in an off-line mode. It includes the required hourly input variables of precipitation, air temperature, dewpoint, incident solar and thermal radiation, albedo, and wind speed. The second will be used to validate model results. Validation variables include ground temperatures, snow depth, snow water equivalent, and snow temperatures at the snow surface and at fixed depths within the pack. Likewise, two models will be run: a baseline model (a version of Abramopoulos et al. 1988) that does not formally model the physics of a snowpack, and a modified model that includes this physics.

TABLE 1. Summary of input and validation datasets available for the NOAA-ARS snow research station.

Variable	Description
Input dataset: Period of record = October 1969–August 1974	
Air temperature (°C)	hourly, taken at 1-m height
Precipitation (m)	hourly, taken at 1-m height
Dewpoint (°C)	hourly, taken at 1-m height
Wind speed (m s ⁻¹)	hourly, taken at 1-m height
Incoming solar (W m ⁻²)	hourly, taken at 1-m height
Reflected solar (W m ⁻²)	hourly, taken at 1-m height when snow is present. Otherwise, albedo is assumed = .15
Incoming longwave (W m ⁻²)	hourly; estimated from Anderson (1967) and clear sky data for site (obtained from Anderson).
Validation dataset: Period of record = October 1969–August 1974	
Snow height (m)	variable (daily to every few days)
Snowpack water equivalent (m)	variable (daily to every few days)
Snow surface temperature (°C)	variable (usually twice daily, 0600 LT and 1800 LT sometimes hourly)
Snowpack temperatures (°C)*	Taken at 6, 12, 24, and 36 in. above ground/snow interface, twice daily (0600 LT and 1800 LT).
Ground temperatures (°C)*	Taken at 3, 6, 12, 24, and 36 in. below ground surface, twice daily (0600 LT and 1800 LT).

* October 1969–August 1973 only.

3. Model descriptions

a. Baseline model

1) MODEL PHYSICS

While Abramopoulos et al. (1988) give an extensive discussion on the baseline land-surface scheme, a brief outline of the ground physics is now given. The model employs a maximum of six separate ground layers, which, in total, extend to a maximum depth of 3.4 m. For most soils the first ground layer thickness is 10 cm. Heat and mass (water) transport are governed by linear diffusion along the thermal gradient and Darcian flow, respectively. The bottom of the sixth layer represents an “impermeable basement” in that there is no heat or mass flow across this boundary. However, as a slope of the ground surface is defined in each grid box sub-surface water may leave a grid box via “pseudo-horizontal” underground runoff. The prognostic variables, heat and water content, are updated each time step. In turn, the fraction of ice and temperature of a layer may then be determined from these variables. While externally driven by hourly meteorological data, the models internal time step is determined from the various stability criteria. Heat and moisture fluxes couple the lower atmosphere to the ground surface. For surface air temperatures less than 0°C, precipitation falls as

snow. Both the heat and moisture content of the snow are then included in the heat and water content of the first ground layer. However, the presence of the snow is not taken into consideration when calculating the thermal conductivity and hydraulic properties of the first layer. Furthermore, the total heat capacity of the first ground layer is taken to be the combined heat capacities of the ground soil in layer 1 and that of the entire snowpack. As such, the only function the snowpack serves in influencing the layer 1 ground temperature is to act as a moisture reservoir. This has a two-fold effect. 1) Dickinson (1988) derives a “surface damping factor,” $d_s = (.5K_{th}C_v\omega)^{1/2}$, where given a heat input of frequency ω , is a measure of the surface temperature response. Using typical values for the thermal properties of soil and snow, diurnal forcing, and the same heat input, Dickinson showed that snow has a surface temperature response an order of magnitude larger than that of soil [i.e., $d_s(\text{snow}) = .1 d_s(\text{soil})$]. However, the baseline model has a higher heat capacity in the first ground layer when snow is present and, thus, always yields a $d_s(\text{snow}) > d_s(\text{soil})$. Therefore, the surface temperature response is unrealistically reduced, and the associated surface energy fluxes are compromised. 2) As no formal snowpack is modeled, the ground is completely uninsulated. For the purposes of calculating surface-atmosphere fluxes, it is as though the ground were directly exposed to the atmosphere, even in the presence of snow cover.

2) MODIFICATION OF THE LOWER BOUNDARY FLUX CONDITION

With a single modification, the baseline model as described above will be used in our validation/improvement experiments. As described above, the treatment of the lower boundary of the ground model as completely insulating is unrealistic. For typical soils, the seasonal temperature variations and, thus, heat flow, reaches as deep as 5–6 m. Neglect of this deep heat flow yields unrealistically large seasonal temperature signals in the lower layers of the model. For a sinusoidal surface temperature forcing in a homogeneous soil, and solving the diffusion equation for temperature gives (Hillel 1980):

$$T(z, t) = \bar{T} + T_s \sin(\omega t - \phi) e^{-z/d}, \quad (1)$$

where

\bar{T} = the mean annual ground temperature

T_s = the maximum amplitude of the surface temperature

$T(z, t)$ = the temperature at depth z and time t

ϕ = the phase shift = $-z/d$

d = the thermal damping depth = $(2K_{th}/(\omega C_v))^{1/2}$

K_{th} = soil thermal conductivity

C_v = soil volumetric specific heat

ω = frequency in radians

z = depth in soil,


and the thermal damping depth, d , is the depth at which the amplitude of the temperature signal is $1/e$ of the surface signal.

For a sandy soil of approximately 40% porosity and volumetric soil moisture of 20% (similar to that found at the snow research station, Fig. 1) the diurnal and annual damping depths are 15.2 cm and 290 cm, respectively (Hillel 1980). At 230.4-cm depth, the deepest model layer is not deep enough to fully resolve the seasonal cycle [Eq. (1)].

Using Eq. (1), the seasonal phase shift between the depths corresponding to midpoints of layers 1 and 6 should be 37 days, and the signal in layer 6 should be damped by 48% relative to the amplitude in layer 1. The model with the no heat flow boundary shows a signal damping of approximately 29% in layer 6 relative to an annual temperature signal applied in layer 1 (Fig. 2a) and a phase shift of 54 days. There are two solutions to this problem. Either increase the number of layers and the total depth of the soil profile to a depth where the no heat flow boundary condition is appropriate, or in some physical manner approximate the effect of heat flow to and from the "deep" to the upper layers. We choose the second solution. The deep is envisioned as a constant heat reservoir at a temperature T_d . Here T_d is taken as the mean annual ground temperature and the no heat flow condition at the base of layer 6 is replaced by the flux condition

$$F_{6,\text{deep}} = -K_6 \frac{dT(z, t)}{dz}, \quad (2)$$

where dT/dz is evaluated at the midpoint of layer 6, $F_{6,\text{deep}}$ is the heat flux between the deep and the sixth layer, and K_6 is the thermal conductivity of layer 6.

0 cm	ATM			Soil Texture*			Nov 1 1969 Initial Conditions	
				% Sand	% Silt	% Clay	Temp (°C)	Theta (%)
10	•	1		65	30	5	1.0	25
25.5	•	2		65	30	5	1.0	25
49.4	•	3		61.1	33.9	5	4.0	19.5
86.1	•	4		56.5	38.5	5	5.4	12.5
	•	5		55	40	5	6.9	17
142.9								
	•	6		55	40	5	8.2	17
230.4								

*Berkshire series

FIG. 1. Model soil profile and 1 November 1969, initial conditions for soil temperature and moisture. Theta is the volumetric soil moisture.

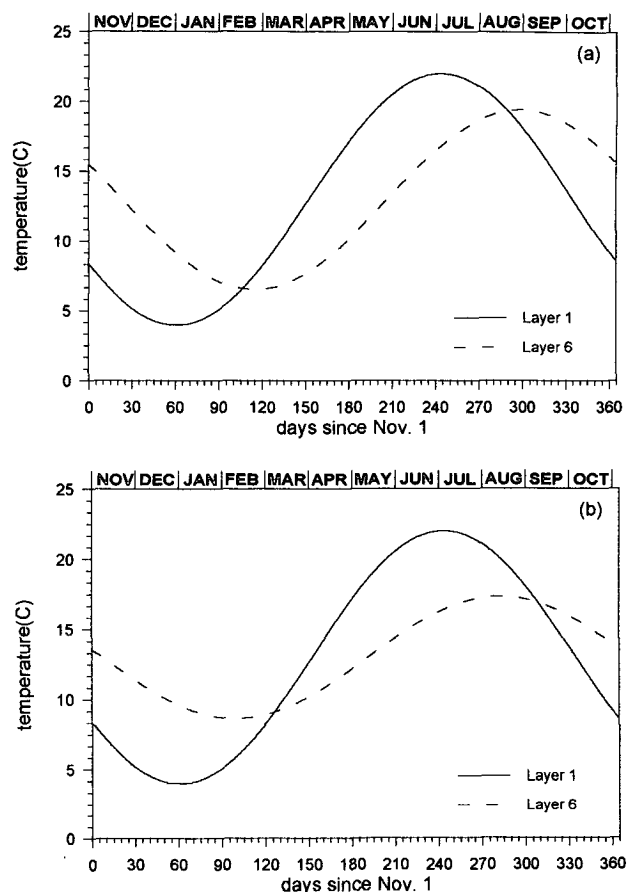


FIG. 2. Model layer 6 temperature response to a layer 1 forcing $T = 13 - 9 \cos(2\pi \text{date}/365)$ where date is the Julian date. (a) Baseline model with the no heat flow boundary condition at the base of layer 6. (b) Baseline model with the layer 6 boundary condition specified by Eq. (5).

The actual temperature gradient, and thus the heat flux, at the base of layer 6 cannot be determined explicitly. From Eq. (1), even in the case of a sinusoidally imposed temperature signal propagating into a homogeneous soil, the temperature gradient, dT/dz , is time dependent:

$$\frac{dT(z, t)}{dz} = -\frac{T_s}{d} [\sin(\omega t - z/d) + \cos(\omega t - z/d)] e^{-z/d}. \quad (3)$$

However, we can approximate this gradient by differencing the temperature of layer 6 from the mean annual temperature and dividing this quantity by an appropriate scaled distance, d' . This yields a flux

$$F_{6,\text{deep}} = -K_6 \frac{(T_6 - T_d)}{d'}, \quad (4)$$

where T_d is the temperature at the depth below which the mean annual signal does not penetrate. The scaling

distance, d' , is determined by minimizing the squared difference between the theoretical value of dT/dz [Eq. (3)] and our approximation for dT/dz [Eq. (4)] integrated over the period of a year. In this manner the scaling distance can be shown to be $d' = d$, the thermal damping depth [Eq. (1)]. The new boundary condition is tested by imposing a sinusoidal temperature signal with a mean annual temperature of 13°C at the midpoint of layer 1. The new boundary condition at the base of layer 6 is

$$F_{6,\text{deep}} = -K_6 \frac{(T_6 - T_d)}{d}, \quad (5)$$

where T_d is taken to be the mean annual value of the imposed surface temperature, 13°C , and the seasonal damping depth, d , of our sandy soil is 2.9 m. This yields (Fig. 2b) a signal damping of 52% and a phase shift of 38 days, reproducing the theoretically predicted damping and phase shift of the seasonal cycle to a high degree of accuracy.

For runs of both the baseline model and the modified snow model, the no heat flow boundary condition is replaced by Eq. (5). Finally, in order to accommodate for climate change experiments in which the mean climate state may change on timescales of longer than one year, the temperature of the deep, T_d , is taken to be the mean running average of the previous years layer 6 temperature. In this way T_d itself becomes interactive.

b. Snowpack model

1) GENERAL COMMENTS

The main characteristic of an insulating material is to limit the otherwise efficient communication between two media. In the case of snow, the two media are the atmosphere and the ground, and the insulator is the snowpack. The effect of the pack is to prevent the escaping of heat from the warm ground to the cold atmosphere, or conversely, to damp out the cold wintertime temperature signal in the snowpack well before it reaches the ground. The low thermal conductivity of snow, about an order of magnitude lower than that of the ground, makes snow an especially good insulator. As such, because snow cover is for the most part seasonal, wintertime ground temperatures remain warmer than they otherwise would be while summertime temperatures are left unaffected. The net result is mean annual ground temperatures greater than the mean annual air temperature in areas where snow cover is significant.

The snowpack is modeled with three snow layers that are numbered 1, 2, 3 from top to bottom. Heat and mass (water) flow within the pack are physically modeled. Radiation conditions determine the surface energy fluxes, and heat flow within the pack is governed by linear diffusion, just as it is in the ground. Each layer is characterized by a volumetric water-holding

capacity. As such, meltwater generated in a layer will remain in the layer if the liquid water content of the layer is less than the layer holding capacity. Otherwise, it will flow down to a lower layer where it will either refreeze in the layer, remain in the layer in the liquid state, or pass through. As the zero reference for heat is taken to be liquid water at 0°C , meltwater flow between layers carries only mass and no heat content. Finally, two independent processes govern densification of the pack. A simple parameterization is used to describe mechanical compaction, or compaction due to the weight of the overburden, and a separate densification is accomplished via the melting-refreezing process.

A key difference between modeling the ground system and a snowpack is that the ground can be described by a set of fixed layer boundaries. As such, a complete description of the system requires only two prognostic variables; layer heat and mass content. The processes of heat and mass flow within the ground layers completely govern changes in these variables. However, as the boundaries of a snowpack move up and down under the influence of snowfall, mechanical and wet compaction, condensation, etc., three variables are needed to completely describe the system; layer thickness (Z_i), mass (W_i), and heat content (H_i). Changes in H_i and W_i are attributed not only to heat and mass flow but also to the fact that the coordinate system describing the snowpack is itself changing. Because layer thicknesses, Z_i , change each time step due to the above processes, a masswise redistribution of heat and mass contents of the three "old" layers and the fresh snow must be performed so the "new" H_i 's and W_i 's correspond to the newly described coordinate system. A similar argument for redistribution can be made for processes leading to snowpack compaction.

2) MODEL PHYSICS

As stated, the model is composed of three snow layers. However, resolution requirements dictate that in order to reasonably capture the diurnal range in the surface radiation temperature, layer 1 thickness can be no greater than the thermal damping depth of snow. As the range of snow diurnal damping depths is 6–10 cm, the following scheme chosen for layer thicknesses is applied at the beginning of each time step:

$$Z_p = \sum Z_i + Z_f \quad (6a)$$

and

$$Z_1^t = .25Z_p^{t-\Delta t} \\ Z_2^t = .50Z_p^{t-\Delta t} \quad \text{for } Z_p \leq .2 \text{ m} \quad (6b)$$

$$Z_3^t = .25Z_p^{t-\Delta t} \\ Z_1^t = .05 \text{ m} \\ Z_2^t = .34(Z_p^{t-\Delta t} - .05) \quad \text{for } Z_p > .2 \text{ m}, \quad (6c) \\ Z_3^t = .66(Z_p^{t-\Delta t} - .05)$$

where Z_i , Z_p , and Z_f are the layer thicknesses, total height of the snowpack after fresh snowfall is taken into account, and the depth of the freshly fallen snow, respectively. These snow heights are chosen to best resolve temperature gradients expected within the pack. The top layer must be thin in order to resolve diurnal fluctuations in the heat content. For a deep snowpack the lowest layer may be thick, as the temperature gradients within the lower part of the pack and between the snow and ground become very small early in the snow season. However, when the snowpack is thin (< 2 m), smaller layers are required at the surface, and in the lowest snow layer where large temperature gradients are expected, especially after a fresh snowfall onto bare soil. Associated with each layer is the mass, given in units of meters as the "water equivalent," W_i , and heat content, H_i , in units J m^{-2} . From these three prognostic variables, Z_i , W_i , H_i , the system is completely described. Layer density can be calculated according to

$$\rho_i = \rho_w(W_i/Z_i), \quad (\text{kg m}^{-3}), \quad (7)$$

where ρ_w is the density of liquid water (kg m^{-3}). Layer thermal properties are then derived:

$$C_v = 1.9 \times 10^6 \rho_i / \rho_{\text{ice}}, \quad [\text{J (m}^3 \text{ K)}^{-1}] \quad (\text{Verseghy 1991}) \quad (8a)$$

$$K_{th} = 3.2217 \times 10^{-6} (\rho_i)^2, \quad [\text{W (m K)}^{-1}], \quad (\text{Yen 1965}) \quad (8b)$$

where $\rho_{\text{ice}} = 920 \text{ kg m}^{-3}$. The temperature, T_i , fraction of ice relative to the total water content in a layer, $f_{l,i}$, and liquid water content in a layer in meters, $W_{L,i}$, can be determined:

$$\begin{aligned} T_i &= 0^\circ\text{C} \\ f_{l,i} &= -H_i / (\rho_w L_f W_i) \quad \text{for } \rho_w L_f W_i + H_i \geq 0; \quad (9a) \end{aligned}$$

$$\begin{aligned} T_i &= (H_i + \rho_w L_f W_i) / (C_{v,i} Z_i) \\ f_{l,i} &= 1.0 \quad \text{for } \rho_w L_f W_i + H_i < 0; \quad (9b) \end{aligned}$$

$$W_{L,i} = (1 - f_{l,i}) W_i, \quad (9c)$$

where L_f is the heat of fusion (J kg^{-1}).

All that remains is to describe those processes that govern changes in the heat content (H_i), mass (W_i), and thicknesses (Z_i) of the layers.

(i) Surface processes

Evaporation/sublimation/condensation. Evaporation, sublimation, and condensation represent sources and sinks of mass and heat into the first snow layer. Evaporation is limited to the liquid water content in layer 1. Here, W_1 is reduced by the amount of evap-

oration, while Z_1 remains unchanged. For sublimation, Z_1 is reduced proportionately to the amount of mass sublimated from the layer. Condensation onto the surface of the pack increases W_1 and Z_1 equally by the amount of condensation. The change in H_1 is given by Eq. (10):

$$\left. \frac{\Delta H_1}{\Delta t} \right|_{\text{latent}} = \lambda \rho_w E_{\text{pot}} = \lambda \rho_w \rho_a C_H V (q_1 - q_s), \quad (10)$$

where

- E_{pot} = potential evaporation rate (m s^{-1})
- λ = heat of vaporization
- ρ_a = density of air
- C_H = bulk transfer coefficient from ground to surface
- V = wind speed
- q_1 = saturated vapor mixing ratio of the first snow layer
- q_s = mixing ratio 1 m above snow surface.

Radiation terms and sensible heat flux. Radiative and sensible heat fluxes directly affect neither the mass nor thickness of layers. Only the heat content is altered via

$$\left. \frac{\Delta H_1}{\Delta t} \right|_{\text{radiative+sensible}} = \sigma (T_1)^4 + C_a \rho_a V C_H (T_1 - T_a), \quad (11)$$

where σ is the Stephan Boltzman constant, C_a is the specific heat capacity of air, and T_a is the surface air temperature. The thermal emissivity of the snowpack is taken to be unity.

Precipitation as rain. For $T_a > 0^\circ\text{C}$, precipitation is in the form of rain. The rainfall imparts its heat content to the heat content of layer 1 and thereafter freezes in layer 1 or flows through the snowpack as meltwater at $T = 0^\circ\text{C}$ appropriately altering W_i of the layers. Here Z_i 's are left unaltered. This meltwater flow through process shall be discussed in detail shortly. The change in H_1 is

$$\left. \frac{\Delta H_1}{\Delta t} \right|_{\text{rainfall}} = C_w \rho_w P_r T_a, \quad (12)$$

where C_w is the specific heat capacity of water and P_r (m s^{-1}) is the precipitation rate for rain.

Precipitation as snowfall. For $T_a < 0^\circ\text{C}$ precipitation falls as snow with a density, $\rho_f = 150 \text{ kg m}^{-3}$. The mass, thickness, and heat content of the fresh snow are

$$\begin{aligned} W_f &= P_s \Delta t \\ Z_f &= (\rho_w / \rho_f) W_f \\ H_f &= (T_a C_{v,f} - \rho_f L_f) Z_f, \quad (13) \end{aligned}$$

where W_f , Z_f , H_f and $C_{v,f}$ are the mass (m), thickness (m), heat content (W m^{-3}), and volumetric specific

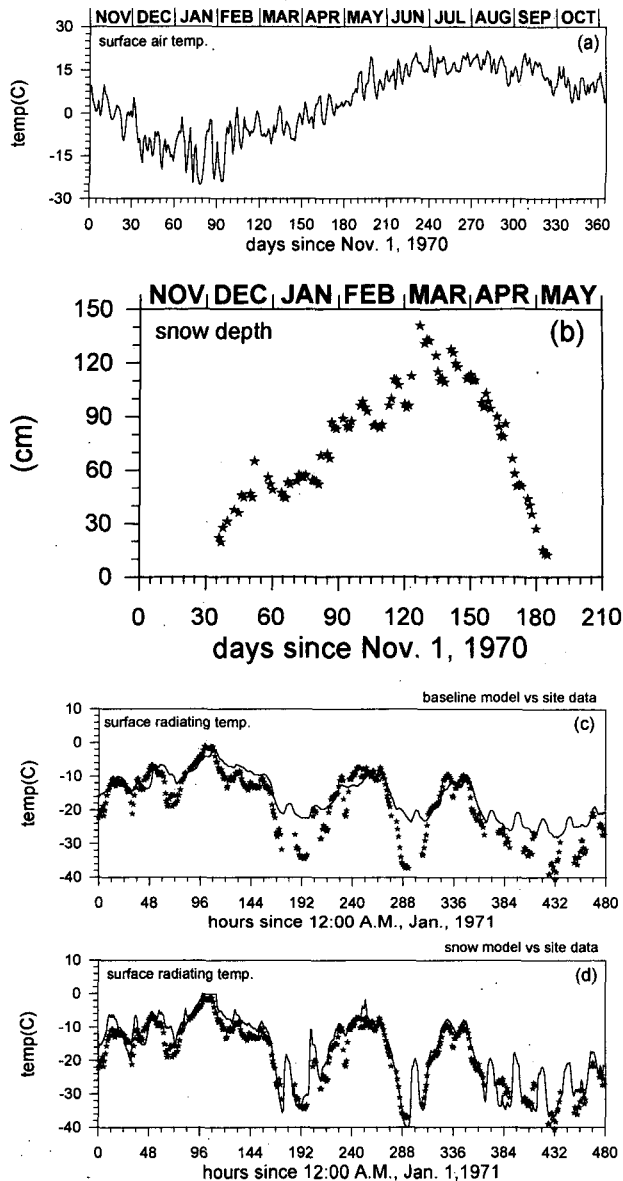


FIG. 3. (a) Air temperature data at 1-m height above surface observed at NOAA-ARS research station. (b) Depth of snowpack observed at NOAA-ARS research station. (c) Hourly surface radiating temperature for 20 days starting 1 January 1971 at NOAA-ARS research station (stars) and predicted by baseline model (solid line). (d) Same as in (c) except solid line is the hourly surface radiating temperature for the snow model. Note that gaps appear in the observed temperature record corresponding to clear, sunny days. The instrument that measures surface radiating temperature overestimates temperature during periods of high insolation, and measurements for these times are discarded.

heat of the fresh snow, respectively. Here P_s is the snowfall precipitation rate (m s^{-1}).

While the above discussion shows how difficult it is to describe the changes in W_i and Z_i with a closed form expression, changes in H_i due to surface processes are amenable to such an expression

$$F_{\text{atm},1} = \left. \frac{\Delta H_1}{\Delta t} \right|_{\text{radiat. + sens.}} + \left. \frac{\Delta H_1}{\Delta t} \right|_{\text{latent}} - \left. \frac{\Delta H_1}{\Delta t} \right|_{\text{precip.}} - I_s - I_{lw}, \quad (14)$$

where $F_{\text{atm},1}$ is the heat flux between the atmosphere and the top snow layer, I_s is the solar heating, and I_{lw} is the atmospheric thermal heating.

(ii) Internal processes

Water flow through. Three processes are now discussed: meltwater generation, layer compaction associated with meltwater generation, and meltwater flow. Given H_i and W_i in each snow layer, the temperature and fraction of ice versus total water in the layers can be calculated using Eq. (9). Should the heat content of a layer exceed the minimum heat necessary to keep the layer entirely frozen, meltwater is generated. In this situation both the layer temperature and meltwater are

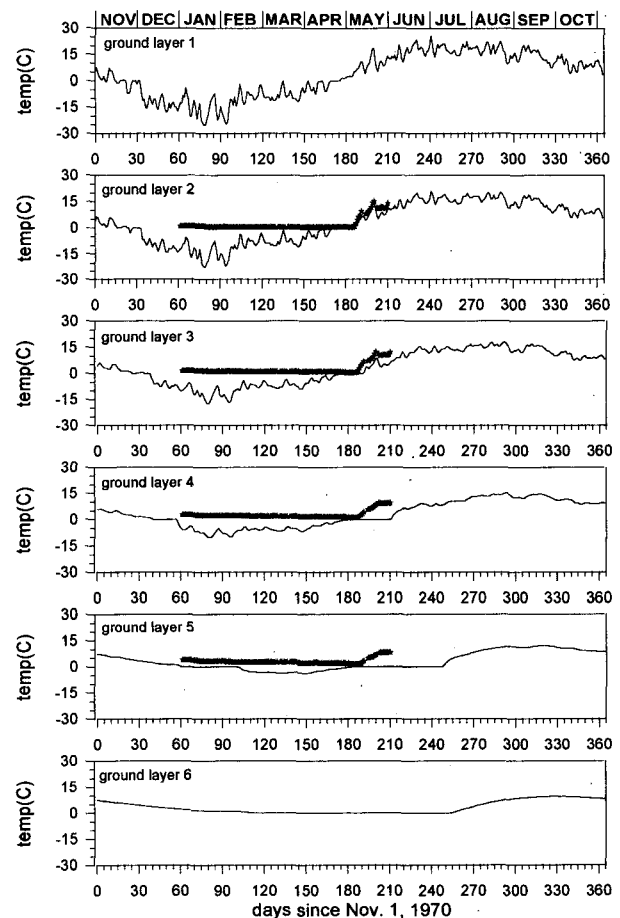


FIG. 4. Daily averaged ground temperatures from year 2 of the baseline model run (solid lines) and ground temperature data observed at the NOAA-ARS snow research station interpolated to the model layer depths (stars).

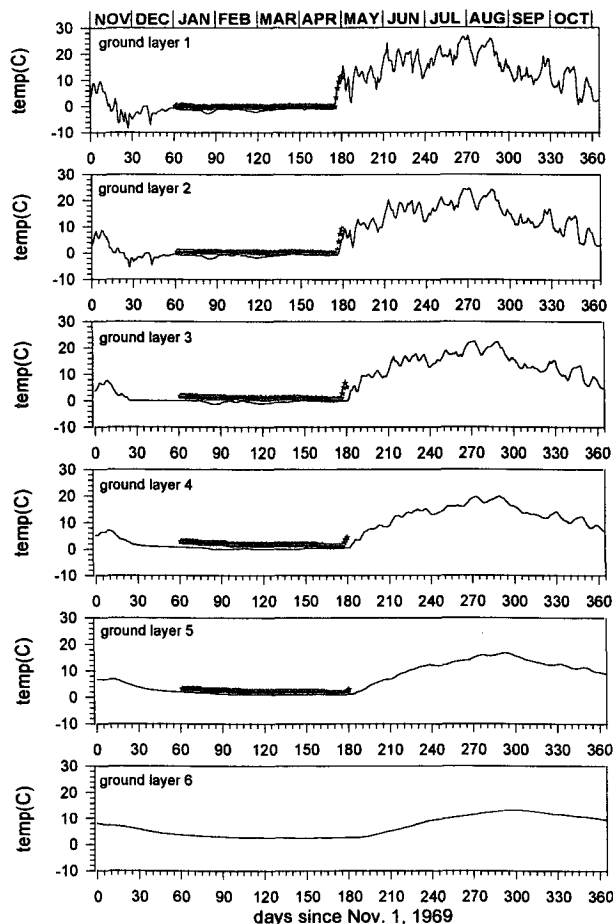


FIG. 5. Daily averaged ground temperatures from year 1 of the snow model run (solid lines) and ground temperature data observed at the NOAA-ARS snow research station interpolated to the model layer depths (stars).

at $T = 0^\circ\text{C}$. This meltwater generation is accompanied by a compaction of the layer thicknesses modeled as

$$Z_i = \left(\frac{f_{1,i}^t}{f_{1,i}^t - \Delta t} \right) Z_i. \quad (15)$$

A liquid water holding capacity is defined for the snowpack and is taken to be 5.5% by height of a compacted layer thickness (Jordan 1991). Should the liquid water content of a layer exceed the layers holding capacity, the excess meltwater flows to the next lowest layer. This mass exchange is reflected in a decrease in W (upper) and a concomitant increase in W (lower). In the lower layer, the liquid water may freeze (depending on the heat and new water content of the lower layer), remain in the lower layer as liquid water, or flow through to the next lowest layer. Liquid water leaving layer 3 of the snowpack is gone from the pack forever and either infiltrates into the ground or leaves the system via surface runoff.

Heat flow. Since meltwater by definition carries zero heat content, heat flow between model layers is accomplished solely via linear diffusion along the temperature gradient according to (Carslaw and Jaeger 1959)

$$F_{i,i+1} = \frac{\Delta H_i}{\Delta t} = - \left(\frac{\Delta Z_i + \Delta Z_{i+1}}{\frac{\Delta Z_i}{K_i} + \frac{\Delta Z_{i+1}}{K_{i+1}}} \right) \left(\frac{T_i - T_{i+1}}{\frac{\Delta Z_i}{2} + \frac{\Delta Z_{i+1}}{2}} \right), \quad (16)$$

where $F_{i,i+1}$ is the heat flux between adjacent snow layers and ΔZ_i is the layer i thickness. The heat flux between the lowest snow layer and the ground is treated in an identical manner. Here Z_i and W_i are not directly affected by heat flow.

Mechanical compaction. The net effect of rainfall and meltwater generation is to densify the pack and, therefore, alter its thermal properties [Eq. (8)]. However, another mechanism that contributes significantly to pack densification is mechanical compaction, which

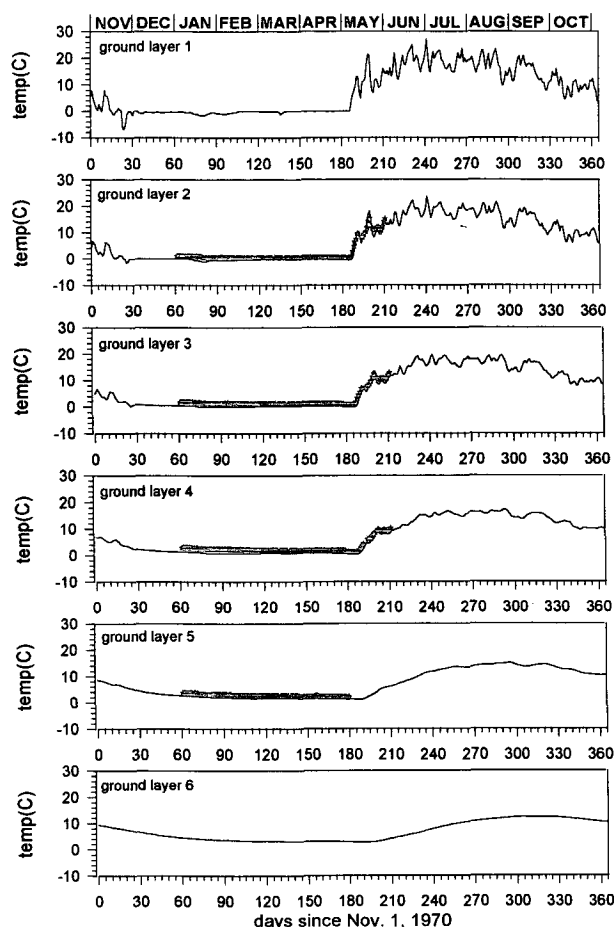


FIG. 6. Daily averaged ground temperatures from year 2 of the snow model run (solid lines) and ground temperature data observed at the NOAA-ARS snow research station interpolated to the model layer depths (stars).

is a self-loading compaction resulting from the weight of the overlying snow. While the microphysics of this compaction is complex, field experiments and modeling by Kojima (1967) have led to development of a simple parameterization that adequately describes the overall effect of this compaction process. Kojima derived equations relating the time rate of change of snowpack density to the vertical stress and viscosity within the pack, as well as relating the viscosity to pack density and temperature. Using these equations and equating the vertical stress to one-half the weight of the pack, Pitman et al. (1991) derived an expression for densification of the pack due to the weight of the overburden. Adapting Pitman's formulation to our three-layer model yields a densification scheme:

$$\rho_i^t = \rho_i^{t-1} + \left\{ .5 \times 10^{-7} \rho_i^{t-1} g N_i \right. \\ \times \exp \left[14.643 - \frac{4000}{\min(T_i + 273.16, 273.16)} \right. \\ \left. \left. - 0.02 \rho_i^{t-1} \right] \right\} \Delta t, \quad (17)$$

where g is the gravitational acceleration and N_i is the mass of the pack above the midpoint of layer i . Results are proportionally applied to the snowpack layers as

$$Z_i = \left(\frac{\rho_i^{t-1}}{\rho_i^t} \right) Z_i. \quad (18)$$

Mechanical compaction leaves H_i and W_i unaffected. Thus, the densification of the snowpack is largely accomplished via three independent mechanisms: mechanical compaction, meltwater generation, and rainfall percolation. Evaporation and condensation will also affect snowpack density in the upper layer to some extent.

3) MODEL STABILITY AND TIME STEP

Although the meteorological data used to drive the model is input hourly, it is the energy fluxes at the surface of the snowpack that mainly determine the model's internal time step. As such, it can be shown that the model time step is proportional to the layer 1 thickness, Z_1 . Therefore, for thin snowcover (typically at the beginning and end of the snow season), an unreasonably short time step is required for model stability. To minimize this problem, the snowpack model is not fully operational before the snow reaches 0.6 cm of water equivalent and ceases to operate once the snow melts to less than this amount. During these periods where the water equivalent is less than 0.6 cm, the snow moisture is "incorporated" into the top ground layer, as in the baseline model (see section 3a.1). During the five snow seasons modeled, the model-determined time step averaged 18 min, with a standard deviation of 9 min. This compares to an average time

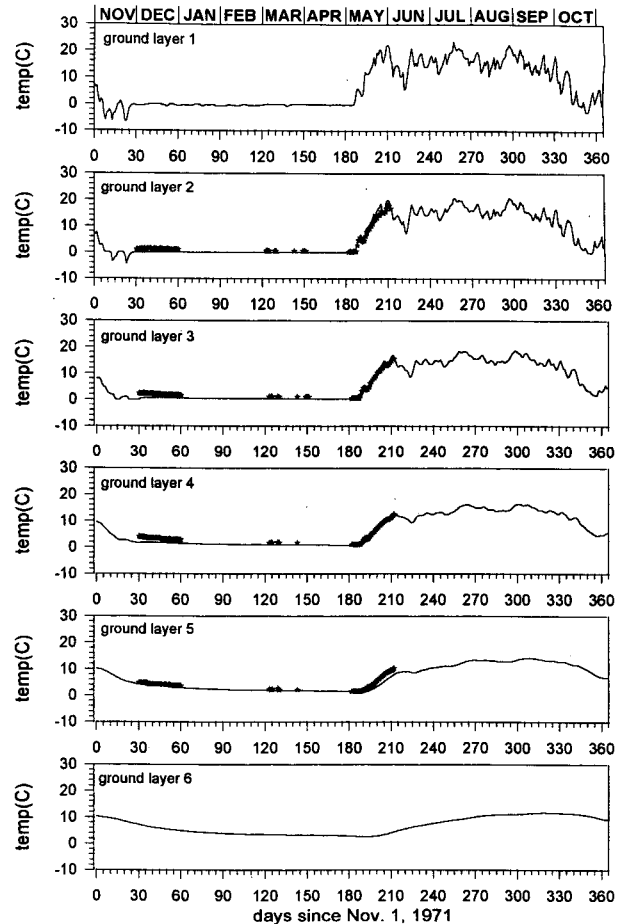


FIG. 7. Daily averaged ground temperatures from year 3 of the snow model run (solid lines) and ground temperature data observed at the NOAA-ARS snow research station interpolated to the model layer depths (stars).

step of 29 min with a standard deviation of 9 min for the baseline model. Due to the shortened time step and added complexity of the new model during the snow season, there was a 22% increase in the 5-year run time compared to the baseline model.

4. Model results

a. Model soil profile and initial conditions

To run the land-surface scheme in an off-line mode, information other than the meteorological input data of Table 1 is required. Soil information must be specified so that soil hydraulic properties can be determined. Likewise, the 1 November 1969 initial conditions for soil moisture and layer temperatures must be given. The predominant soil at the NOAA-ARS snow station is of the Berkshire series (USDA 1993). Surface pressure at the site is taken to be 950 mb, the mean station value. The average ground slope of the W-3 watershed, 8%, was selected as the models specified ground slope.

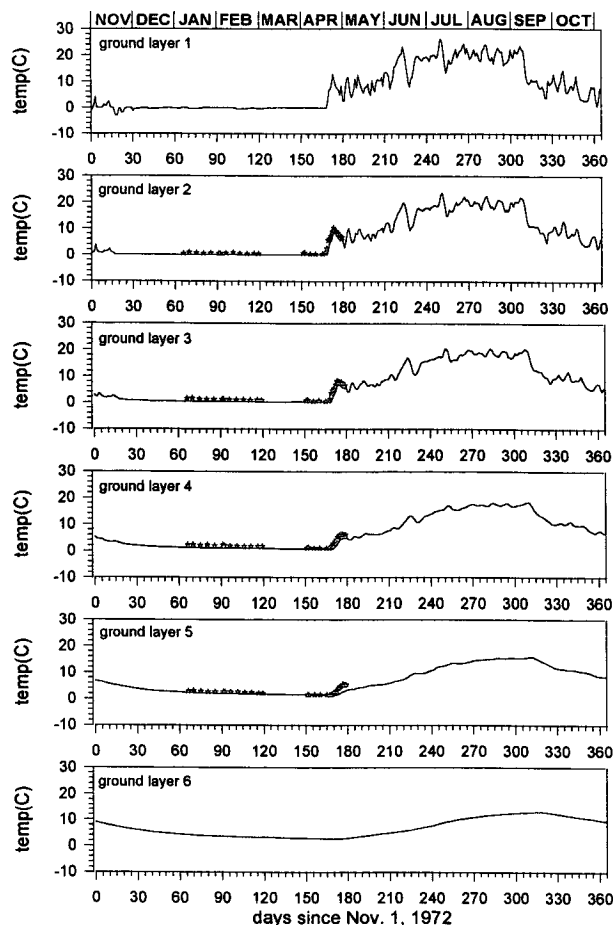


FIG. 8. Daily averaged ground temperatures from year 4 of the snow model run (solid lines) and ground temperature data observed at the NOAA-ARS snow research station interpolated to the model layer depths (stars).

Initial volumetric moisture was determined from the site soil moisture record and initial ground temperatures were estimated from the long-term air temperature record at the site and the solution of the diffusion equation over a semi-infinite halfspace with respect to a sandy soil. The model soil profile with the 1 November 1969 ground moisture and temperatures are shown in Fig. 1. The maximum depth of the soil profile is determined by the FAO database (1974). Finally, these runs are for bare soil only and do not model the effects of vegetation.

b. Baseline model results

To generate the 1 November 1969 initial condition for the temperature of the deep, T_d , a 16-year spinup run was performed. Using the first four years of meteorological input data (1 November 1969–30 September 1973), the soil profile and initial conditions of Fig. 1, and an assigned initial $T_d = 4.1^\circ\text{C}$, the long-

term mean air temperature at the snow research station, the baseline model was spun up for 16 years by cycling through the input data four times. Climatology was considered achieved when the mean annual layer 6 ground temperatures for the years in a cycle equalled the corresponding temperatures for years in the previous cycle. After three cycles the model reached a “steady state” and the 1 November 1969 T_d was taken to be the average layer 6 temperature generated in years 13–16. Here T_d determined in this manner was 3.17°C . Since both theory and experimental data show that on a long-term basis $T_d \geq \bar{T}_a$, the fact that $T_d(\text{baseline}) < \bar{T}_a$ by 1°C is an early indication that by not formally modeling the physics of the snowpack the baseline model generates surface fluxes inconsistent with the meteorological input data.

To evaluate the behavior of the baseline model the full five years of meteorological data are now used to generate model results. As all five years of model–data comparisons yielded the same general story; only results from one year are presented. Figures 3a–c and Fig. 4 present data and model results for the period 1 November 1970–30 September 1971. Since the baseline

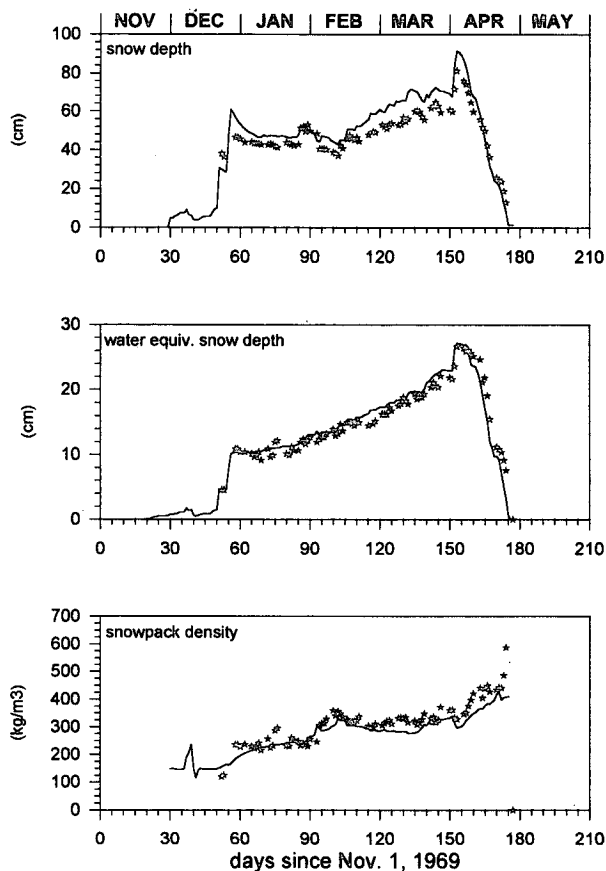


FIG. 9. Model-predicted snow depth, water equivalent snow depth (mass), and snowpack density for year 1 (solid line) and observed snow characteristics at the NOAA-ARS research station (stars).

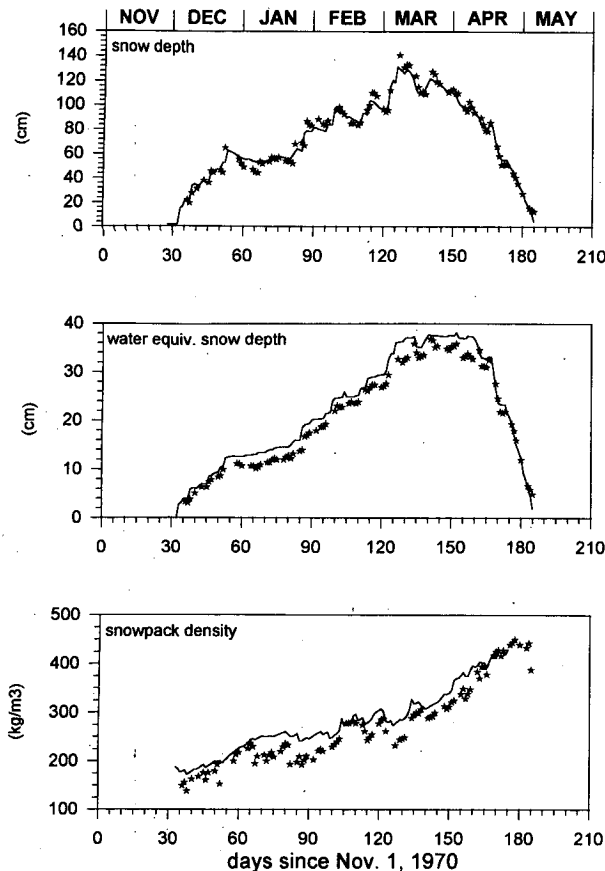


FIG. 10. Model-predicted snow depth, water equivalent snow depth (mass), and snowpack density for year 2 (solid line) and observed snow characteristics at the NOAA-ARS research station (stars).

scheme does not model the snowpack itself, only comparisons of ground temperatures are used to evaluate model behavior. However, an appreciation for the insulation properties of a snowpack can be obtained by first examining the site data. While the 1970–1971 winter air temperatures regularly drop below 20°C , ground temperatures remain at or above 0°C . Snow cover, which is appreciable from 7 December to 5 May, limits the heat flux from the ground to such an extent that below 7.5 cm the ground is never frozen and by the end of the spring melt the ground is entirely thawed.

Baseline model results give an entirely different picture. Figure 4 shows the large cooling effect of large wintertime heat fluxes from the noninsulated ground. Not only do surface ground temperatures dip into the -20°s , but ground layers freeze to a depth of 2 m. With model volumetric soil moisture at approximately 25%–35%, this freezing represents such a large heat loss to the system that deeper layers do not unfreeze until midsummer. The effects of this spatially deep and temporally long-lasting freezing are many. As the main characteristic of frozen soil is to “lock up” the otherwise available water content, Darcian flow is completely in-

terrupted. Drainage in winter out of deep layers is impossible. Runoff/infiltration from spring melt and spring–summer rainstorms cannot be properly calculated. The mass transport of water from deep layers that would otherwise support high rates of spring–summer evaporation/transpiration is prohibited. It is the lack of sufficient treatment of the snowpack that is responsible for the inconsistent surface heat fluxes that lead to large ground cooling. This is revealed in the curves depicting model-data surface radiation temperatures (Fig. 3c). On extremely cold days the high thermal conductivity and heat capacity of the first ground layer lead to a damped thermal response with model surface temperatures 15°C too warm. As surface radiative cooling is proportional to T^4 , the ground layers are artificially cooled. The above discussion demonstrates that the effects on hydrologic processes due to the presence or absence of snow cover are not solely confined to the winter but are felt throughout the year. As such, the inability of the baseline model to distinguish between snow cover and non-snow cover situations impacts the year-round model calculations of runoff/infiltration, internal heat and mass flow, evap-

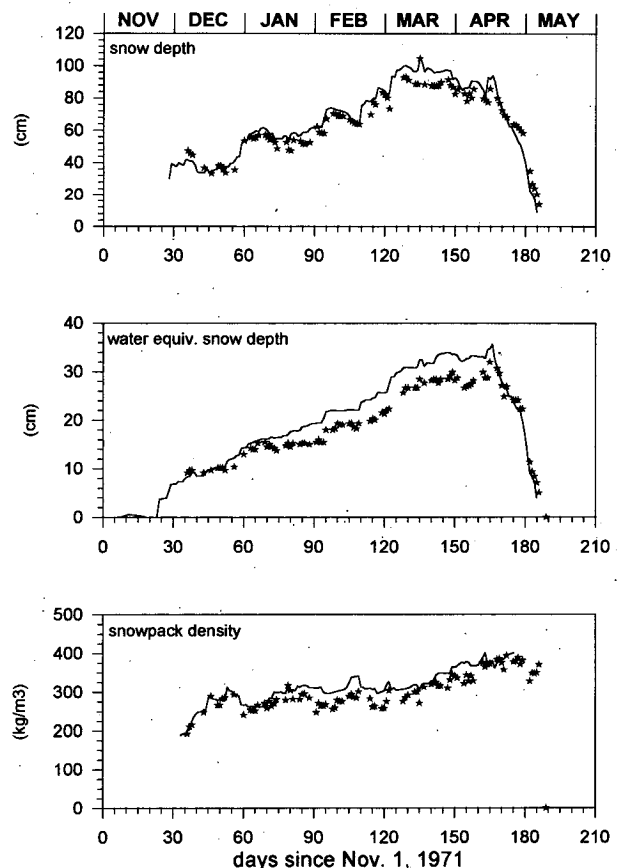


FIG. 11. Model-predicted snow depth, water equivalent snow depth (mass), and snowpack density for year 3 (solid line) and observed snow characteristics at the NOAA-ARS research station (stars).

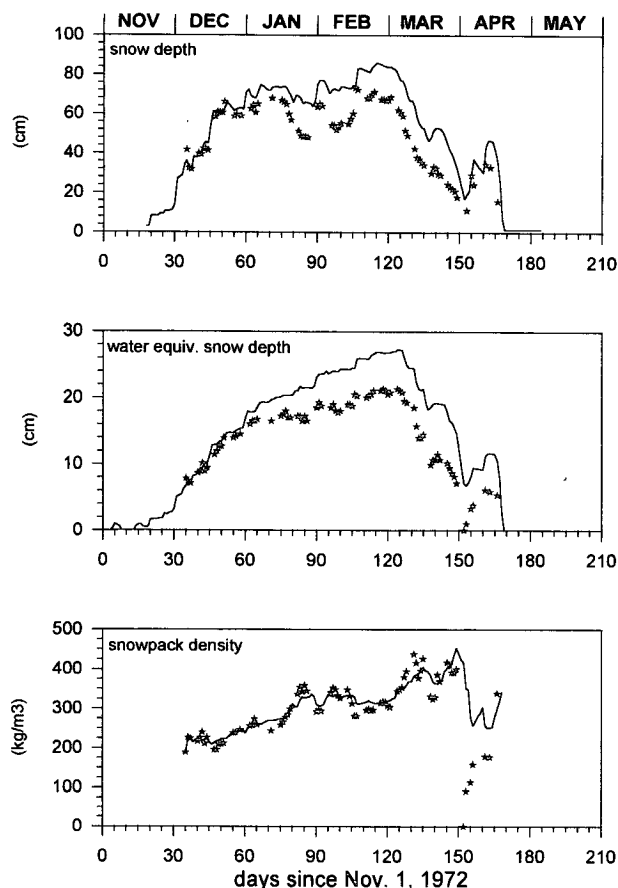


FIG. 12. Model-predicted snow depth, water equivalent snow depth (mass), and snowpack density for year 4 (solid line) and observed snow characteristics at the NOAA-ARS research station (stars).

oration/transpiration, and the surface radiating temperature.

c. Snow model results

This newly developed snow model was run with the same soil profile and initial conditions (Fig. 1) as in the baseline run. To determine the 1 November 1969 initial condition for the temperature of the deep, the snowpack model was spun up as described for the baseline model. The T_d determined in this manner was $T_d = 6.46^\circ\text{C}$. The fact that $T_d > \bar{T}_a$ by 2.5°C reflects the asymmetric nature of snowpack insulation in that the ground is insulated from the atmosphere only in winter. The full five years of meteorological data were then used to generate model results that could be compared with site data. Figures 3d and 5–14 present model–data comparisons for ground temperatures, snowpack growth/ablation and density, and snow surface temperatures.

For all four years in which comparisons can be made, model ground temperatures show remarkable agree-

ment with site data. This includes the post-snowpack springtime recovery of temperatures in the upper layers.

The five years of model–data comparisons of snowpack growth/ablation and densification also show good agreement. As reflected in the snowpack density and water equivalent snow depth curves (or the single composite curve of snow depth), most melting events and the final snowpack collapse in each year are captured adequately. The model even seems robust, although less so, for the highly variable 1973/74 snow season. While the overall patterns of growth/ablation during the 1972/73 and 1973/74 snow seasons are resolved, there is a clear trend for model overestimation of water equivalent snow depth during these years. Two possible explanations are offered. As opposed to the 1969/1972 snow seasons, which can be characterized as dry, cold years in which precipitation fell almost exclusively as snowfall and there was little midseason melting, the 1972/73 and especially the 1973/74 snow season are characterized by numerous warm rain on snow events. These rain on snow events aid in the development of vertical channels (Kattlemann 1989) forming within the pack that act as preferred outflow

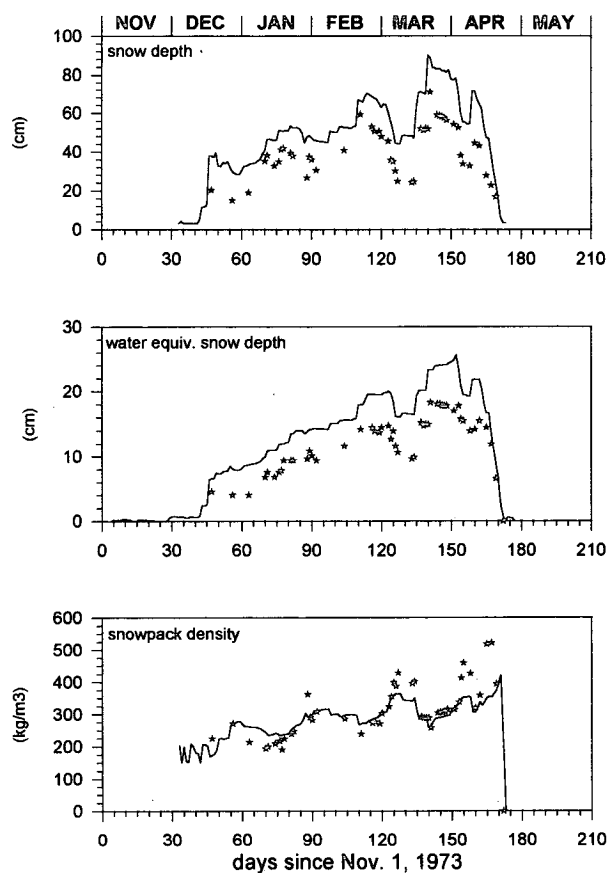


FIG. 13. Model-predicted snow depth, water equivalent snow depth (mass), and snowpack density for year 5 (solid line) and observed snow characteristics at the NOAA-ARS research station (stars).

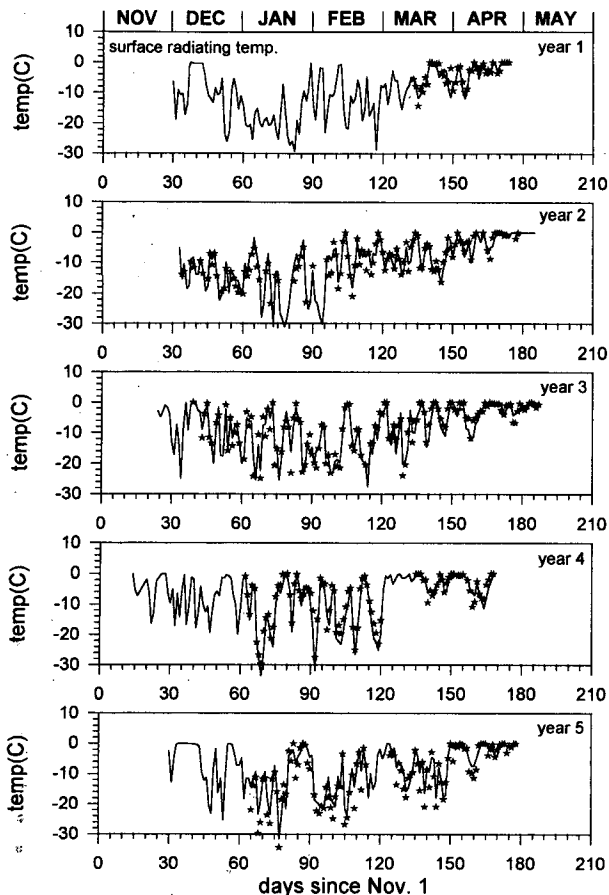


FIG. 14. Five years of daily averaged modeled (solid lines) and observed (stars) snow surface radiating temperatures.

pathways for meltwater generated in the pack and rain falling on the pack. Likewise, these years are characterized by ice-layer unconformities that prevent vertical flow and instead route water horizontally out of the pack to the downslope regions of the research station (Anderson 1976). While both of these processes lead to the efficient routing of meltwater/rainwater out of the pack, neither is modeled.

As temperature is a direct reflection of heat and mass content [Eq. (9)], the model's ability to properly account for heat and mass flow within the pack can be evaluated by comparing model-data snow-layer temperatures. Both on hourly (Fig. 3d) and daily (Fig. 14) timescales the model reproduces the surface radiation temperature quite well. As such, model-generated surface fluxes are consistent with the meteorological input data. While not shown, model-data comparisons for internal snowpack temperatures also show good agreement. All the processes that characterize snowpack "ripening" are reproduced by the model. This ripening, as observed in nature, is characterized as follows. Toward the middle/end of the snow season meltwater generated near the top of the pack percolates into the

pack and freezes at lower levels (the models equivalent of wet compaction). The net effect of this mass transport is to raise the temperature of lower layers, eventually leading to the development of an isothermal pack at $T = 0^{\circ}\text{C}$. This preconditions the pack for its very rapid springtime collapse. In combination with the gradual buildup of snow over the winter this rapid collapse yields a sawtooth-like growth/ablation curve.

Finally, it is worthwhile examining how well the model captures the seasonal subsurface temperature signal. However, between May and November site ground temperature data do not exist. Furthermore, the theoretical calculations of a 37-day phase lag and a 48% damping of the seasonal signal between model layers 1 and 6 can be considered only lower limits. Equation (1) does not include the effects of liquid water to ice phase transitions within the ground. Therefore, ground temperature data from Bozeman, Montana, a site similar to Sleepers River in terms of cold climate and prolonged winter snow cover is used in lieu of data for our site. Despite the differences in soil type and the possibility for differences in the soil moisture content at the two sites, Fig. 15 indicates that the model produces results reasonably consistent with observed data. While the similarity between upper-layer temperatures (the forcing) may be coincidental, the similarity of the lower-layer temperature responses requires either that the model is working consistently or that there is an infortuitous compensation between the model's failures and differences in the thermal and moisture properties at the two sites.

5. Conclusions

Five years of meteorological and hydrological data from a typical New England watershed where winter snow cover is significant were used to drive and validate two off-line land-surface schemes; a baseline scheme that did not model the physics of a snowpack, and therefore, neglected the insulating properties of snow

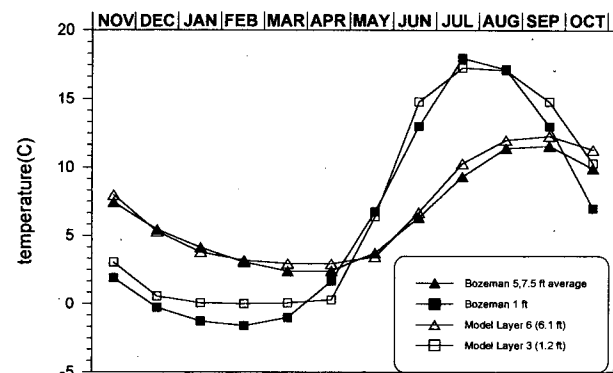


FIG. 15. Observed monthly averaged ground temperatures at Bozeman, Montana, (Chang 1958) and monthly averaged ground temperatures from year 2 of the snow model run (see Fig. 6).

cover, and a modified scheme in which a three-layer snowpack is modeled. Comparing the baseline model results with validation data revealed several model deficiencies. Surface radiation temperatures could not adequately be modeled and the ground froze to unreasonable depths. Further, because of ground cooling resulting from large surface heat fluxes to the atmosphere from the uninsulated surface, deeper model layers did not unfreeze until midsummer. As such, the normal hydrologic processes of runoff, ground water infiltration and movement, etc. are interrupted for a good part of the year. With the inclusion of a simple three-layer snow model into the baseline model, not only are the ground and surface radiation temperatures adequately modeled, but all the features of snowpack ripening that characterize pack growth/ablation are simulated.

Now that a model has been developed that captures the winter/spring ground freezing/thawing at the site, the model's behavior with respect to other hydrologic processes can be studied. Currently, our three-layer snow model has been incorporated into the physics of the baseline model for bare soil conditions only. As the Sleepers River watershed is 100% vegetated (excluding the snow research station) it is necessary to couple the snow model physics into the entire baseline model, including the portions that deal with vegetated ground. Using site validation data of soil moisture and watershed runoff, our new model can then be evaluated and improved with respect to rainfall/runoff/infiltration relationships. This will be the focus of the next paper.

Acknowledgments. I thank D. Rind, C. Rosenzweig, F. Abramopoulos, J. Lynch-Stieglitz, and R. Jordan, for their many helpful discussions. I also thank E. Anderson at the National Weather Service Hydrologic Research Laboratory, R. Dekett at the USDA Soil Conservation Service, T. Pangburn at the Cold Regions Research and Engineering Laboratory, and J. Thurman at the USDA-ARS Hydrology Laboratory for supplying the datasets and soil maps used in this study. This work was supported by the U.S. Environmental Protection Agency office of Exploratory Research and office of Policy, Planning, and Evaluation, Global Climate Change Division.

REFERENCES

- Abramopoulos, F., C. Rosenzweig, and B. Choudhury, 1988: Improved ground hydrology calculations for global climate models (GCMs): Soil water movement and evapotranspiration. *J. Climate*, **1**, 921–941.
- Aguado, E., 1985: Radiation balances of melting snow covers at an open site in the Central Sierra Nevada, California. *Water Resour. Res.*, **21**, 1649–1654.
- Anderson, E. A., 1967: Estimating incident terrestrial radiation under all atmospheric conditions. *Water Resour. Res.*, **3**, 975–988.
- , 1976: A point energy balance model of a snow cover. Office of Hydrology, National Weather Service, NOAA Tech. Rep. NWS 19.
- , 1977: NOAA-ARS cooperative snow research project—Watershed hydro-climatology and data for water years 1960–1974. NOAA Tech. Rep., NOAA—S/T 77-2854.
- Barnett, T. P., L. Dumenil, U. Schlese, E. Roeckner, and M. Latif, 1989: The effect of Eurasian snow cover on regional and global climate variations. *J. Atmos. Sci.*, **46**, 661–685.
- Carslaw, H. S., and J. C. Jaeger, 1959: *Conduction of Heat in Solids*. 2d ed. Oxford University Press, 510 pp.
- Chang, J.-H., 1958: *Ground Temperatures*. Vol. 2. Harvard University Press, 196 pp.
- Charney, J. G., 1975: Dynamics of deserts and drought in the Sahel. *Quart. J. Roy. Meteor. Soc.*, **101**, 193–202.
- , W. K. Quirk, S.-H. Chow, and J. Kornfield, 1977: A comparative study of the effects of albedo changes on drought in semi-arid regions. *J. Atmos. Sci.*, **34**, 1366–1385.
- Deardorff, J. W., 1978: Efficient prediction of ground surface temperature and moisture with inclusion of a layer of vegetation. *J. Geophys. Res.*, **83**, 1889–1903.
- Dickinson, R. E., 1988: The force-restore model for surface temperatures and its generalizations. *J. Climate*, **1**, 1086–1097.
- , A. Henderson-Sellers, P. J. Kennedy, and M. F. Wilson, 1986: Biosphere-Atmosphere Transfer Scheme (BATS) for the NCAR Community Climate Model. NCAR Tech. Note NCAR/TN-275+STR, 69 pp.
- FAO-UNESCO, 1974: Soil Map of the World 1:5,000,000. UNESCO, Paris.
- Hillel, D., 1980: *Fundamentals of Soils Physics*. Academic Press, 413 pp.
- Jordan, R., 1991: A one-dimensional temperature model for a snow cover. U.S. Army Corps of Engineers, Cold Regions Research and Engineering Laboratory, Special Report 91-16, 49 pp.
- Kattlemann, R., 1989: Spatial variability of snow-pack outflow at a site in Sierra Nevada, USA. *Ann. Glaciol.*, **13**, 124–128.
- Kojima, K., 1967: Densification of seasonal snow cover. *Physics of Ice and Snow, Proc. Int. Conf. on Low Temperature Science*, Sapporo, Japan, Institute of Low temperature Science, Hokkaido University, 929–952.
- Namias, J., 1985: Some empirical evidence for the influence of snow cover on temperature and precipitation. *Mon. Wea. Rev.*, **113**, 1542–1553.
- Pitman, A. J., Z.-L. Yang, J. G. Cogley, and A. Henderson-Sellers, 1991: Description of bare essentials of surface transfer for the Bureau of Meteorological Research Centre AGCM, BRMC, Australia. BMRC Research Report No. 32, 117 pp.
- USDA, 1993: Soil maps of the W-3 watershed and soil interpretation records. Soil Conservation Service, Caledonia County, VT.
- Verseghy, D. L., 1991: CLASS—A Canadian land surface scheme for GCMs. I: Soil model. *Int. J. Climatol.*, **11**, 111–133.
- Yeh, T.-C., R. Wetherald, and S. Manabe, 1983: A model study of the short term climatic and hydrological effects of sub-snow cover removal. *Mon. Wea. Rev.*, **111**, 1013–1024.
- Yen, Y. C., 1965: Heat transfer characteristics of naturally compacted snow. U.S. Army Cold Regions Research and Engineering Laboratory, Research Report 166, Hanover, NH, 9 pp.